arXiv:cond-mat/0304224v1 [cond-mat.stat-mech] 9 Apr 2003

# Free energy calculations of elemental sulphur crystals *via* molecular dynamics simulations

C. Pastorino and Z. Gamba

Department of Physics, Comisión Nacional de Energía Atómica CAC,

Av. Libertador 8250, (1429) Buenos Aires, Argentina. *

(Dated: 2nd February 2008)

## Abstract

Free energy calculations of two crystalline phases of the molecular compound $S_8$ were performed *via* molecular dynamics simulations of these crystals. The elemental sulphur $S_8$ molecule model used in our MD calculations consists of a semi-flexible closed chain, with fixed bond lengths and intra-molecular potentials for its bending and torsional angles. The intermolecular potential is of the atom-atom Lennard-Jones type. Two free energy calculation methods were implemented: the accurate thermodynamic integration method proposed by Frenkel and Ladd [1] and an estimation that takes into account the contribution of the zero point energy and the entropy of the crystalline vibrational modes to the free energy of the crystal. The last estimation has the enormous advantage of being easily obtained from a *single* MD simulation. Here we compare both free energy calculation methods and analyze the reliability of the fast estimation *via* the vibrational density of states obtained from constrained MD simulations. New results on α- and α'-$S_8$ crystals are discussed.

*Electronic address: clopasto@cnea.gov.ar, gamba@cnea.gov.ar.

## I. INTRODUCTION

In recent papers we studied the crystalline phases of the molecular compound $S_8$, the most abundant natural form of elemental sulphur around ambient pressure and temperature (STP). Three crystalline allotropes of this compound are known: $\alpha$-$S_8$ phase is orthorhombic with 16 molecules in the non-primitive unit cell [2, 3]. If several samples of this crystal are slowly heated, some of them will show a phase transition to $\beta$-$S_8$ at 369 K, which in turn melts at 393 K [2], but most of them show a metastable melting point at 385.5 K [2, 3]. Monoclinic $\beta$-$S_8$ is usually obtained from the melt [2] and has 6 molecules per primitive unit cell, two of them orientationally disordered above 198 K [4]. Monoclinic $\gamma$-$S_8$ has four molecules in a pseudo-hexagonal close packed unit cell, with a density 5.8% higher than $\alpha$-$S_8$ at STP [3].

Using a very simple molecular model consisting of a cyclic semi-flexible chain of 8 atoms, with constant S-S bond lengths, it is possible to reproduce many features of the complex phase diagram of the $S_8$ molecule [6, 7]. The intra-molecular potential model includes a harmonic bending potential for S-S-S angles and a double well for the torsional angles [8], the intermolecular potential used was a simple *Lennard-Jones* non-bonded atom-atom interaction, the details and potential parameters are given in the Section III. Using this simple interaction model we could reproduce, via a series of classical constant temperature- constant pressure simulations [6, 7], the following experimental facts: the crystalline structure, the configurational energy and the lattice, bending and torsional dynamics (as given by the calculated density of vibrational modes) of $\alpha$-, $\beta$- and $\gamma$-$S_8$ for T$\geq$200 K; the orientational dynamical order - disorder phase transition of $\beta$-$S_8$ and, finally, the solid-liquid phase transition of a cubic disordered sample was calculated near the experimental value [6, 7].

Nevertheless, we found a fact that cannot be reproduced by this simple molecular model [6, 7]: when the temperature of a $\alpha$-$S_8$ MD sample of 288 molecules is lowered below 200 *K*, our orthorhombic $\alpha$-$S_8$ sample shows a structural phase transition to a monoclinic phase, with a molecular array similar to that of $\alpha$-$S_8$ and that we called $\alpha'$-$S_8$ [7]. This has not been experimentally observed. This spontaneous change was most probably due to the large fluctuations associated to a relatively small sample. A larger sample of 512 molecules didn't show this distortion, but its configurational energy and volume per molecule remained, nevertheless, higher than those calculated for $\alpha'$-$S_8$ [7]. Fig. 1 shows both structures and the configurational energy vs. temperature, that of $\alpha$-$S_8$ was calculated by slowly decreasing T in steps of 25 to 50 K. The same study for $\alpha'$-$S_8$

is performed by increasing T, after a long stabilization and annealing to obtain a totally ordered structure at the starting point of 50 K, this is the reason for the different $U_{conf}$ values, in fig. 1, at this point. Experimental measurements of the $\alpha$-$S_8$ structure at 300 and 100 K clearly disregard a structural phase transition, unless a metastable state has been experimentally measured [9, 10], and this fact shows the limits of applicability of the simple molecular model.

In refs. [7, 11] we analyzed if an anisotropic non- bonded atom-atom intermolecular potential model was able to reproduce all the experimental facts. Using the program GAMESS [12], we performed *ab initio* calculations of the electronic density distribution of the $S_8$ molecule, and the measured anisotropy of this distribution around each atom due to the atomic lone pairs. The calculated electronic density reproduces the experimental crystalline measurements of Coppens *et. al.* [13], with a lone pair center at 0.7Å of the S location; nevertheless, at the nearest crystalline distances found between non-bonded atoms, the atomic anisotropy is low. The MD simulations performed with this anisotropic potential did not improve the previous result (shown in Fig. 1), unless a quite unrealistic atomic anisotropy is used [11, 14].

It has to be pointed out that the search of a reliable molecular model for elemental sulphur molecules is extremelly useful due to the practical impossibility of performing quantum mechanical simulations of the complex phase diagram of these molecular crystals, with a large number of atoms in the primitive cells.

In this paper we decided to implement a reliable calculation of the free energy of $\alpha$-$S_8$ and $\alpha'$-$S_8$ crystals in order to review the conclusions obtained with the first molecular model [6, 7], based on an estimation of the free energy that takes into account the contribution of the vibrational modes to the zero point energy and entropy of the sample [6, 7]. Our present calculations are useful to check our previous free energy estimations and, at the same time, for the comparison of both free energy calculation methods. The usefulness of this comparison is due to the fast way in which the free energy can be estimated, within the quasi-harmonic approximation, using the data of a single MD simulation.

In the following sections we give the details of the implemented free energy calculations, the inter- and intra-molecular potential model used, the performed MD simulations, the obtained results and our conclusions.

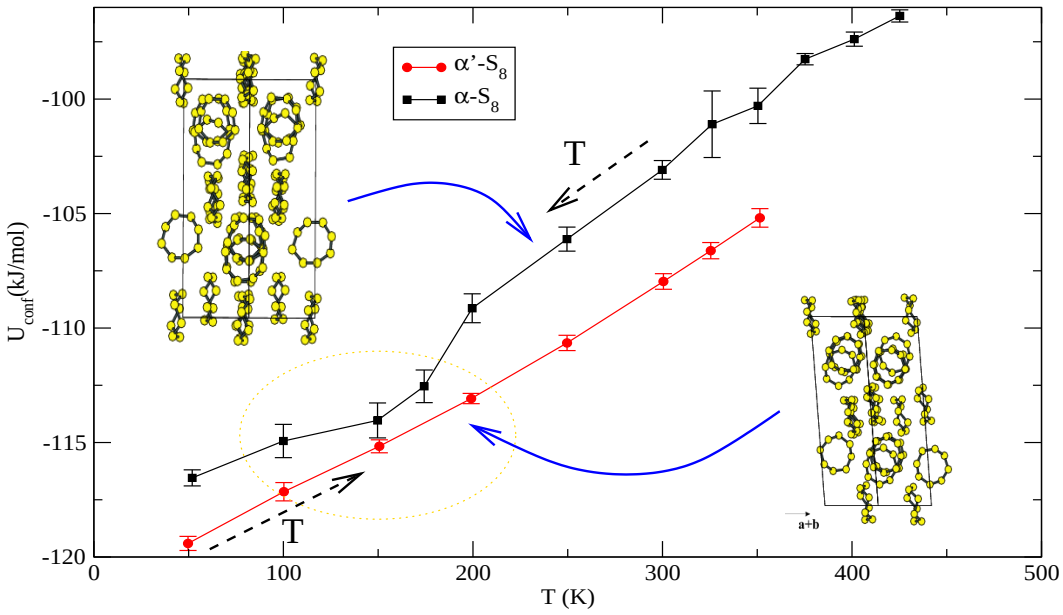


Figure 1: Configurational energy of α and α'-$S_8$ as obtained in ref. [6]. The structural transition to α'-$S_8$ is observed spontaneously below $200\,K$.

## II. FREE ENERGY CALCULATIONS

In order to obtain reliable free energy values we implemented the thermodynamic integration method of Frenkel and Ladd [1], including the two correction terms given in refs. [15, 16]. From the results of a single MD simulation, we also estimated the free energy in the quasi-harmonic approximation, that is usually employed in lattice dynamics calculations [17]. In Section IV we give the details of our performed MD simulations.

### A. Thermodynamic integration method

This method proposes a thermodynamic integration along a reversible path between the system we are interested in and another one for which the free energy can be analytically calculated [1, 15, 16]. For crystalline samples the reference system is an Einstein crystal, for which the internal energy is calculated as:

$$U_{Einstein} = U(\{\mathbf{r}_0^N\}) + \sum_{i=1}^{N} \alpha(\mathbf{r}_i - \mathbf{r}_0)^2 \,,$$

where $\{\mathbf{r}_0^N\}$ is the set of coordinates of the minimum energy configuration (the equilibrium atomic

coordinates) and $U(\{\mathbf{r}_0^N\})$ its potential energy, the second term is the harmonic potential energy of the N oscillators. The force constant $\alpha$ is taken equal for all degrees of freedom and its value, $\alpha$ =18.0844 kJ/mol, is chosen so as to obtain a mean square displacement equal to the average one in the real crystal: $\langle \Delta r^2 \rangle_{Einstein} \sim \langle \Delta r^2 \rangle_{real}$. The potential energy difference between the real and the reference crystals can be calculated along a reversible artificial pathway that links both systems. At any intermediate point of the path, given by the coordinate $\lambda$ $(0 \leq \lambda \leq 1)$, the local value of $U$ is

$$\widetilde{U}(\lambda) = U(\{\mathbf{r}_0^N\}) + (1-\lambda)[U(\{\mathbf{r}^N\}) - U(\{\mathbf{r}_0^N\})] + \lambda \sum_{i=1}^{N} \alpha(\mathbf{r}_i - \mathbf{r}_0)^2 . \quad (1)$$

So, for $\lambda = 0$ the potential energy of the real crystal is recovered and, for $\lambda$=1 the potential energy is that of the Einstein crystal:

$$\widetilde{U}(\lambda = 0) = U_{sist}$$

and

$$\widetilde{U}(\lambda = 1) = U_{Einstein} .$$

The free energy difference between the real and the reference crystal is given by [1, 16]:

$$F(\lambda = 0) - F(\lambda = 1) = -\int_0^1 d\lambda (\frac{\partial F(\lambda)}{\partial \lambda}) = -\int_0^1 d\lambda \langle \frac{\partial \widetilde{U}(\lambda)}{\partial \lambda} \rangle_\lambda ,$$

and deriving eq. 1:

$$F = F_{Einstein} + \int_{\lambda=1}^{\lambda=0} d\lambda \left\langle \sum_{i=1}^{N} \alpha(\mathbf{r}_i - \mathbf{r}_0)^2 - [U(\mathbf{r}^N) - U(\mathbf{r}_0^N)] \right\rangle_\lambda . \quad (2)$$

The free energy of the Einstein crystal, with a fixed center of mass for the MD sample, is [18]:

$$\frac{F_{Einstein}}{N} = U(\mathbf{r}_0^N) - \frac{3(N-1)}{2N\beta} \ln(\frac{2\pi}{\alpha\beta}) - \frac{3\ln N}{2N} - \frac{\ln V_0}{\beta N} + 3\ln(\Lambda) , \quad (3)$$

where $\Lambda = \frac{h}{\sqrt{2\pi m k_B T}}$ is the de Broglie thermal wavelength , $\beta = \frac{1}{k_B T}$, $N$ is the number of atoms and $V_0$ is the equilibrium volume of the sample.

If $N_{mol}$ is the number of molecules of the system, the final expression, including a correction term due to the center of mass constraint of the sample [1, 16, 18] and a second correction term due to its finite size [15], is:

$$\frac{\beta F}{N_{mol}} = 3\frac{N}{N_{mol}}\ln(\Lambda) - \frac{3(N-1)}{2N_{mol}}\ln(\frac{2\pi}{\beta\alpha}) - \frac{3\ln(N)}{2N_{mol}} - \frac{\ln V_0}{N_{mol}} - \frac{\beta}{N_{mol}}\int_0^1 \langle U_{ein} - U\rangle_\lambda \,. \qquad (4)$$

The accuracy of this calculation is determined by a correct evaluation of the last term in eq. 4, where long MD simulations are needed to measure the integrand for each value of $\lambda$.

For all values of $\lambda$, the center of mass of the sample is held fixed at the origin because the 'springs' of the reference Einstein crystal are tied to the equilibrium atomic positions. This is important to avoid divergences of the integrand in eq. 4 when $\lambda$ is close to 0 [1, 16].

The third term in eqs. 3 and 4 includes the change of the sign mentioned in ref. [15], with respect to the original work of Frenkel and Ladd [1], due to a new consistent calculation of the partition function of the constrained CM system [15]. This term is negligible in a large system but must be taken into account to compute absolute free energies of a typical MD sample.

### B. Quasi-harmonic approximation

Following Born and Huang [17], the free energy of a harmonic crystal with $N_d$ degrees of freedom ( i. e. $N_d$ independent harmonic oscillators) can be calculated as:

$$F = \sum F_i = U_{conf} + \frac{1}{2}\sum_{i=1}^{N_d} h\nu_i + k_B T \sum_{i=1}^{N_d} \ln(1 - e^{-\frac{h\nu_i}{k_B T}}), \qquad (5)$$

where $U_{conf}$ is the potential energy and the $\nu_i$ are the vibrational frequencies of a system with $N_d$ degrees of freedom.

We have implemented this method, as in ref. [6, 7], in two steps. First we calculate the atomic velocities self correlation function $C(t)$, using the MD data stored in a free trajectory in the phase space of the sample:

$$C(t) = \frac{\langle v(t).v(0)\rangle}{\langle v(0).v(0)\rangle},$$

where <> imply averages over atoms and over different initial times.

In a second step we calculate the vibrational density of states $D(\nu)$ *via* a Fourier transform of $C(t)$, and replace the sums over frequencies in eq. 5 by an integral on frequencies, weighted by the calculated density of vibrational modes. We have to take into account that the normalization factor for $D(\nu)$ is such that $\int D(\nu)\, d\nu = N_d$. In our case is $N_d = 16N_{mol}$, because we have 8 bond constraints per molecule.

We can then calculate the internal energy, the entropy and free energy as [17]:

$$F = U_{conf} + \frac{1}{2}\int d\nu D(\nu)\, h\nu + k_B T \int d\nu D(\nu)\, \ln(1 - e^{-\frac{h\nu}{k_B T}})\,, \tag{6}$$

$$S = -(\frac{\partial F}{\partial T})_V = \int \frac{e^{-\frac{h\nu}{k_B T}}}{1 - e^{-\frac{h\nu}{k_B T}}} \frac{h\nu}{T} D(\nu) d\nu\,,$$

$$U = F - TS = U_{conf} + \frac{1}{2}\int d\nu D(\nu)\, h\nu + \int \frac{e^{-\frac{h\nu}{k_B T}}}{1 - e^{-\frac{h\nu}{k_B T}}} \frac{h\nu}{T} D(\nu) d\nu\,.$$

The approximations involved in our quasi-harmonic calculations, with the results of a single MD simulation, are the following:

- $U_{conf}$ is calculated by performing averages, over time and molecules, of the potential energy per molecule calculated in the MD run, $U_{conf} =< U >$, it is not the value of the minimum potential energy $U_0$ of the Einstein crystal in equation 3.

- The calculated vibrational density of states $D(\nu)$ of the MD crystalline sample, due to its finite size ( a few number of primitive unit cells are included in it) does not give an accurate measurement of the density given by the real dispersion curves, the frequencies are only measured in a few points of the reciprocal space.

- The anharmonic frequencies of the sample can be accurately measured with a MD simulation, but eq. 6 is called the 'quasi-harmonic' approximation because eq. 5 is exact only for harmonic potentials.

## III. INTRA- AND INTERMOLECULAR POTENTIAL MODEL

The potential model is that of refs. [6, 7]. The flexible molecular model includes all low frequency molecular distortions that mix with lattice modes and can therefore be of relevance in a possible structural phase transition. The S-S bond distances are kept constant ($d_{SS} = 2.0601$ Å) because the stretching modes are well above in energies ($\nu > 400\, cm^{-1}$) than the rest of the vibrational modes ($\nu < 250 cm^{-1}$).

We must stress here that bond constraints can have nonnegligible contributions to the free energy calculations. Such contributions have been studied elsewhere , with different methods and

techniques [19, 20, 21]. The main conclusions of those explicit calculations, using both MD [19] and MCTI [20], are that the influence of bond constraints is actually negligible when the bond length is not changed from the initial to the final state. This is the case in our $S_8$ phases, in which the primitive cell will change and the molecules will distort from one phase to the other but the molecules bond length is held fixed within the same value for every calculation presented in this work. If changes in bond length between initial and final states of the free energy calculation were involved, an explicit constraint contribution to the free energy must be considered as explained in refs. [20, 21]. For the sake of completeness, a simple estimation of the change in the probability density between the standard $NVT$ and the 'bond-constrained' ensemble of $S_8$ is given in the Appendix.

The bending intramolecular potential for S-S-S angles is harmonic [8],

$$V(\beta) = \frac{1}{2} C_\beta (\beta - \beta_0)^2$$

with a force constant of $C_\beta$=25725 $k_B$/rad$^2$ and $\beta_0$= 108 deg. The intramolecular potential for torsion angles is a double well [8],

$$V(\tau) = A_\tau + B_\tau \cos(\tau) + C_\tau \cos^2(\tau) + D_\tau \cos^3(\tau),$$

with $A_\tau$=57.192 k$_B$, $B_\tau$=738.415 k$_B$, $C_\tau$=2297.880 k$_B$ and $D_\tau$=557.255 k$_B$. These parameters describe a double well with minima at $\tau$=180 $\pm$ 98.8 deg., and a barrier height of about 9 kJ/mol at $\tau$=180 deg. The barrier height at $\tau$=0 deg. is of 30 kJ/mol, out of the range of energies explored in these simulations.

The intermolecular potential is of the non-bonded atom-atom Lennard-Jones type, with parameters $\varepsilon$=1.70 kJ/mol and $\sigma$=3.39 Å [6, 8]. The cut-off radius of the interactions is 15 Å and correction terms, to the energy and pressure, due to this finite cut-off are taken into account by integrating the contribution of an uniform distribution of atoms for distances larger than our cut-off of 15 Å.

## IV. MOLECULAR DYNAMICS SIMULATIONS

The MD simulations and samples are entirely identical to those previously performed in refs. [6, 7]. The bond constraints are held fixed with the SHAKE algorithm [22] and the temperature

is maintained using the Nosé-Hoover chains method [23], although the same behavior was found using the standard Nosé method [24, 25] in our NPT ensemble simulations.

Taking the equilibrated samples of α- and α'-$S_8$ from our simulations in refs. [6, 7] as starting point, we first did a careful measurement of their crystalline structures (i. e. the lattice parameters and volume $V_0$) by averaging the calculated values over long runs performed in the NPT ensemble. The time step of the simulations was of 0.01 ps, the thermalization of the samples was of 80000 time steps (800 ps) and they were measured in the following 30000 (300 ps) time steps. The lattice parameters of each one of the four samples, together with their averaged atomic positions, were taken as the equilibrium atomic locations for the corresponding Einstein crystals.

The next series of MD simulations, as a function of the λ parameter $(0 < \lambda < 1)$, were performed at constant volume, with a standard time step of 0.005 ps and runs of 160000 time steps (800 ps) of thermalization followed by a 40000 time steps (200 ps) of a free trajectory in the phase space, that were used to measure the systems.

For λ values close to 1, we had to reduce the time step up to a minimum of 0.0001 ps in order to obtain the same accuracy in the total energy as for the other values of λ. Accordingly, the total number of time steps were increased so as to accumulate nearly the same total time of thermalization and storage of the other cases.

As in refs. [18, 26], ten values of the parameter λ are defined by a ten point Gauss-Legendre quadrature method, used to resolve the thermodynamic integration on the λ coordinate (last term en eq. 4).

## V. RESULTS

### A. Thermodynamic integration method

Fig. 2 shows the values of $U_{free}(\lambda) = \langle U_{Einstein} - U \rangle_\lambda$, obtained with averages over the lasts 200 ps of each run, for α- and α'-$S_8$ at 300 K. Similar curves $U_{free}(\lambda)$ are calculated for α− and α′-$S_8$ at 100K, except that for $\lambda \sim 1 < U_{free} >$ is about −260 kJ/mol. For both temperatures the values for the α′-$S_8$ sample are systematically lower than those of α-$S_8$, the difference increases for increasing values of λ.

Note that the values $U_{free}(\lambda)$ near $\lambda \sim 1$ are those that weight more in the calculation of the integral in eq. 4. $\lambda \sim 1$ implies strong springs of Einstein crystals and weak interactions of the

original system, in this case the slope of $< U_{free}(\lambda \sim 1) >$ has a large increment because each atom is subjected almost only to the harmonic force of the Einstein crystal, allowing molecular configurations very different from those of the real system. Each atom shows a mean square displacement that depends only on temperature and not in the forces of the real system. At higher temperatures the interactions are more repulsive (because of the shorter mean interatomic distances) and $< U_{free} >$ takes more negative values ($U$ has a negative sign in the integrand of eq. 4). This can be verified noting that for $T = 100$ K the minimum $< U_{free} >$ is approximately $-260$ kJ/mol, almost half the value at 300 K (-510 kJ/mol, see figure 2).

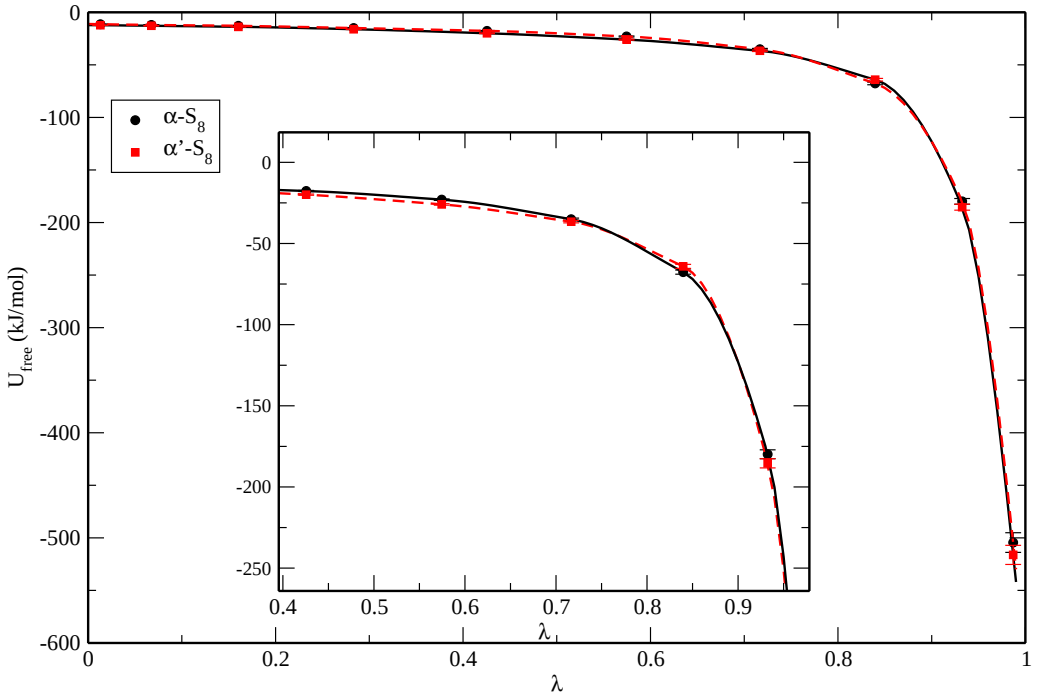


Figure 2: $\langle U_{free} \rangle$ for $\alpha-$ and $\alpha'$-$S_8$ at 300K. Each point is a MD run. This curve is the integrand of the last term in equation 4, from which the free energy is obtained using the Frenkel Ladd thermodynamic integration scheme . The lines are a guide to the eyes and were calculated with the Akima interpolation algorithm.

The contributions of the different terms to the total free energy of eq. 4, in adimensional units, are included in Table I. The first three rows present the same values for all the cases, the first two of them are large terms that almost cancel each other. The next three rows show the terms that are calculated different in each case, and are obtained from the MD simulation data. The main contributions are from the $U_0$ static term and from the thermodynamic integration term. In the last

row the adimensional free energy values for all the cases are shown.

| Phase/Temp. | $\alpha$-$S_8$ $(T = 100K)$ | $\alpha'$-$S_8$$(T = 100K)$ | $\alpha$-$S_8$ $(T = 300K)$ | $\alpha'$-$S_8$ $(T = 300K)$ |
|---|---|---|---|---|
| $3\frac{N}{N_{mol}}\ln\Lambda^*$ | -1162.78 | -1162.78 | -1162.78 | -1162.78 |
| $-\frac{3(N-1)}{2N_{mol}}\ln(\frac{2\pi}{\beta\alpha^*})$ | 1148.94 | 1148.94 | 1148.94 | 1148.94 |
| $-\frac{3\ln(N)}{2N_{mol}}$ | -0.04032 | -0.04032 | -0.04032 | -0.04032 |
| $\beta U_0$ | -143.05 | -146.08 | -46.91 | -48.47 |
| $-\frac{\ln(V_0^*)}{N_{mol}}$ | -0.02529 | -0.02529 | -0.02540 | -0.02535 |
| $-\frac{\beta}{N_{mol}}\int_0^1 d\lambda\,\langle U_{ein}-U\rangle_\lambda$ | 25.1(4) | 25.5(4) | 21.3(4) | 22.0(4) |
| $\frac{\beta F_{einstein}}{N_{mol}}$ | -143.79 | -146.63 | -47.65 | -49.22 |
| $\frac{\beta F}{N_{mol}}$ | -131.41 | -133.97 | -39.05 | -39.91 |

Table I: Contribution of the different terms to the free energy value, calculated by the thermodynamic integration method for both temperatures and phases. For the sake of comparison each term has been adimensionalized using the definitions $\Lambda^* = \Lambda/\sigma$, $\alpha^* = \alpha\sigma^2$ and $V_0^* = V_0/\sigma^3$ when needed.

The integral for thermodynamic integration in eq. 4 was also calculated using numerical integration for the Akima interpolation curve (see figure 2) and the difference with the Gauss-Legendre quadrature is within 6.4 %. The error of this term, included in table I was obtained with the same Gauss-Legendre quadrature using the values $U_{free}(\lambda)+\Delta U(\lambda)$ and $U_{free}(\lambda)-\Delta U(\lambda)$, where $\Delta U$ is the statistical error of each MD simulation.

There is a further comment about this free energy calculation method and its use in systems with multiple constraints, as are the very commonly used semiflexible molecular models with bond length constraints. In our simulations the constraints were not only applied to the real systems but also to the corresponding Einstein crystals. In this way we computed free energy differences between two constrained systems (the real and the reference) for each one of the four studied cases. This is irrelevant as long as we compare the free energy between the $\alpha$- and $\alpha$'-$S_8$ crystals or between them and their reference systems. However, when computing the absolute free energy of each crystal, it has to be taken into account that the bond length constraints affect its MD trajectory in the phase space . The correction terms for systems with multiple types of constraints were recently discussed by Otter and Briels [27], they found that the bond constraint contribution is not negligible only when comparing systems of different bond lengths [19, 20, 21].

### B. Quasi-harmonic approximation

The absolute values of the free energies of the four samples were also calculated *via* the contribution of the density of vibrational modes $D(\nu)$ to the entropy and zero point energy of the sample. With the measurement of an unique run in the *NPT* ensemble, for each one of the four real systems, we obtained the values included in Table II. The samples are equilibrated and measured at a pressure of $0.\pm 0.03$ kbar and the *pV* term is not included to allow a direct comparison with the thermodynamic integration method. The volume per molecule $(V_m)$, configurational energy ($U_{conf}$), zero point energy ($E_{Q_0}$), entropy ($S$) and free energy ($F$) are shown. The free energy calculated with this approximation for various temperatures between 100 and 300 K, not included here, showed a systematically lower values for α'-$S_8$.

| Phase | α-$S_8$ **(**$T = 100K$**)** | α′-$S_8$**(**$T = 100K$**)** | α-$S_8$ **(**$T = 300K$**)** | α′-$S_8$ **(**$T = 300K$**)** |
|---|---|---|---|---|
| $\langle V_m \rangle$(Å$^3$) | 196.8(3) | 196.0(3) | 203.1(4) | 201.2(2) |
| $\langle U_{conf} \rangle$(kJ/mol) | -114.6(1) | -116.7(1) | -105.5(3) | -108.96(3) |
| $E_{Q_o}$(kJ/mol) | 16.083 | 16.285 | 15.950 | 15.836 |
| $TS$(kJ/mol) | 4.3929 | 4.2900 | 26.6491 | 26.9034 |
| $F$(kJ/mol) | -102.4(3) | -103.9(3) | -123.2(1.3) | -126.0(1.2) |

Table II: Different quantities involved in the free energy calculations *via* the density of vibrational modes. $E_{Q_o}$stands for the zero point energy term.

### C. Comparison of both methods

Table III includes the calculated absolute values of free energy, in kJ/mol units, for α− and $\alpha' - S_8$ at 100 and 300 K, using both methods.

We expect higher accuracy in the absolute free energy values for the thermodynamic integration method, mainly at higher temperatures when the harmonic approximation is worst than in the case of 100 K, due to the fact that anharmonic effects are expected to increase at higher temperatures.

With the thermodynamic integration method the difference of free energies is calculated about $\Delta F_{\alpha-\alpha'}(T = 300K) \sim 2\,\frac{kJ}{mol}$ , being α'-$S_8$ the more stable phase. Although the absolute free energy values are not similar, the difference between both phases is also of about 2 kJ/mol for the

| $\mathbf{T}=100\mathbf{K}$ | $\mathbf{F}_{TI}(\mathbf{kJ/mol})$ | $\mathbf{F}_{QH}(\mathbf{kJ/mol})$ | $\mathbf{T}=300\mathbf{K}$ | $\mathbf{F}_{TI}(\mathbf{kJ/mol})$ | $\mathbf{F}_{QH}(\mathbf{kJ/mol})$ |
|---|---|---|---|---|---|
| $\alpha$-$S_8$ | -109.3(4) | -102.4(3) | $\alpha$-$S_8$ | -130.0(1.0) | -123.2(1.3) |
| $\alpha'$-$S_8$ | -111.(3) | -103.9(3) | $\alpha'$-$S_8$ | -132.4(1.0) | -126.0(1.2) |

Table III: Comparison of the absolute free energy values using thermodynamic integration (TI) and Quasi-harmonic approximation (QH).

quasi-harmonic method. This difference can be experimentally measured and closely follows that between the corresponding $U_0$ and $U_{conf}$ included in table IV.

| Phase | $T(K)$ | $\mathbf{F}_{TI}(\mathbf{kJ/mol})$ | $\mathbf{F}_{QH}(\mathbf{kJ/mol})$ | $U_0(kJ/mol)$ | $U_{conf}(kJ/mol)$ |
|---|---|---|---|---|---|
| $\alpha$-$S_8$ | 100.3(1.9) | -109.3(4) | -102.4(3) | -118.936 | -114.6(1) |
| $\alpha'$-$S_8$ | 100.8(1.9) | -111.39(34) | -103.94(25) | -121.461 | -116.7(1) |
| $\alpha$-$S_8$ | 299.6(5.1) | -130.27(96) | -123.2(1.3) | -117.008 | -105.5(3) |
| $\alpha'$-$S_8$ | 300.9(4.9) | -132.4(1.0) | -126.0(1.2) | -120.901 | -108.0(3) |

Table IV: Comparison of the free energy values for the thermodynamic integration and the quasi-harmonic approximation methods. The values of the energy for the mean positions ($U_o$) and the mean configuration energy ($U_{conf}$) are also shown for the two phases and the two studied temperatures.

## VI. CONCLUSIONS

In this paper we calculated the free energy of orthorhombic $\alpha$-$S_8$ crystals and compared it with that of monoclinic $\alpha$'-$S_8$ [6, 7, 11, 14], a previously proposed phase that is calculated with lower mean volume per molecule and lower potential energy than $\alpha$-$S_8$ crystals. The monoclinic $\alpha$'-$S_8$ crystal was obtained in the course of MD simulations, using simple inter- and intramolecular potential models, but has not been experimentally observed [9, 10]. Therefore, in this work we performed an accurate measurement of the free energy difference between both crystals at 100 and 300 K (above and below the spontaneous transition found in ref. [6]), as given by the simple molecular model of [6]. The thermodynamic integration method [1, 15] is implemented, taking as reference system the corresponding Einstein crystals. For the sake of comparison we also included calculations of the free energy in the quasi-harmonic approximation, a fast estimation method that can be easily implemented in MD simulations.

The accurate free energy calculations performed here still show that monoclinic α'-$S_8$ is calculated more stable than the orthorhombic experimentally observed α-$S_8$, in accord with our previous calculations [6, 7] performed with the same simple molecular model and in the quasi-harmonic approximation.

As regards the accuracy of the free energy calculations, we found that for the thermodynamic integration method the results are extremely sensitive to the accurate calculation of the values $U(\lambda)$. In particular for $\lambda \sim 1$ long MD simulations are needed. Although the absolute free energy values differ for both calculation methods, both measure a difference of about 2 kJ/mol between α- and α'-$S_8$ crystals, being α'-$S_8$ the more stable.

The approximated method for calculating the free energy *via* the contribution of the vibrational modes to the energy and entropy of the system turns out to be very useful to determine relative values between polymorphic phases or between different temperatures of a given sample. This result is very important, taking into account that this method is, at least, ten times faster than the thermodynamic integration method, that requires at least ten lengthly MD simulations (one MD run for each value of the λ parameter), in order to calculate the free energy of one sample at a given temperature.

**Acknowledgments**

C. P. thanks Ignacio Urrutia for fruitful and encouraging discussions as regards bond constrains in free energy calculations and FOSDIC for a partial support. This work was partially supported by the grant PIP 0859/98 of CONICET and Fundación Balseiro-2001.

## I. APPENDIX

We estimate here the difference in the calculated statistical averages for MD simulations performed with and without molecular bond length constraints. This topic has been extensively treated in literature and is not of minor importance [16, 28, 29, 30]. Indeed, it has been widely studied in the case of free energy calculations that involve a reaction coordinate [29, 30].

We recall the results of chapter 10 from ref. [16] and the appendix from ref. [28]. The expression for the ratio of molecular position probability for constrained and unconstrained system is:

$$\frac{\rho(\mathbf{q}_1,...,\mathbf{q}_{3N})}{\rho(\mathbf{q}_1,...,\mathbf{q}_{3N-l},\mathbf{q}_1^c=\sigma_1,...,\mathbf{q}_l^c=\sigma_l)} = c\sqrt{|Z|}\,, \tag{1}$$

where we explicitly note the constrained degrees of freedom with $\mathbf{q}_i^c = \sigma_i$, being the standard bond length constraint,

$$\sigma_i = \sqrt{m_i}(\sqrt{\mathbf{r}_{ij}^2} - d \equiv 0)\,, \tag{2}$$

and $l$ constrained bonds are assumed. The $l \times l$ $Z$ matrix, in the right hand side of 1 is defined as [16, 28]:

$$Z_{mn} = \sum_{i=1}^{N} \frac{1}{m_i}(\frac{\partial\sigma_m}{\partial\mathbf{r}_i}).(\frac{\partial\sigma_n}{\partial\mathbf{r}_i})\,, \tag{3}$$

and $||$ stands for the determinant. The origin of $Z$ is from the fact that not only $\sigma(\mathbf{r}_i) = 0$ must be required to constraint the bonds in the simulations, but also $\dot{\sigma}(\mathbf{r}_i) = 0$ at all times [30]. It should be noted that $\mathbf{q}$ in eq. 1 is used for generalized coordinates while $\mathbf{r}_i$ for cartesian ones.

For the $S_8$ molecule we have 24 degrees of freedom, from which 8 have been constrained in our model (see sec. III). Therefore we have 16 degrees of freedom with 8 bond constraints following eq. 2, with $d$ =2.06 Å. Matrix $Z$ can be explicitly calculated for a $S_8$ molecule from eq. 3:

$$\begin{pmatrix}
2 & \cos(\beta_{12}) & 0 & 0 & 0 & 0 & 0 & \cos(\beta_{18}) \\
\cos(\beta_{12}) & 2 & \cos(\beta_{23}) & 0 & 0 & 0 & 0 & 0 \\
0 & \cos(\beta_{23}) & 2 & \cos(\beta_{34}) & 0 & 0 & 0 & 0 \\
0 & 0 & \cos(\beta_{34}) & 2 & \cos(\beta_{45}) & 0 & 0 & 0 \\
0 & 0 & 0 & \cos(\beta_{45}) & 2 & \cos(\beta_{56}) & 0 & 0 \\
0 & 0 & 0 & 0 & \cos(\beta_{56}) & 2 & \cos(\beta_{67}) & 0 \\
0 & 0 & 0 & 0 & 0 & \cos(\beta_{67}) & 2 & \cos(\beta_{78}) \\
\cos(\beta_{18}) & 0 & 0 & 0 & 0 & 0 & \cos(\beta_{78}) & 2
\end{pmatrix},$$

where $\beta_{ij}$ is the bending bond angle between consecutive angles $i$, $j$ and $j+1$.

If we take a mean $\beta$ value for all the bending angles and evaluate the determinant in eq. 1, we get:

$$|Z| = 256 - 576\cos(\beta)^2 + 400\cos(\beta)^4 - 88\cos(\beta)^6\,. \tag{4}$$

We can now take a statistical mean value over the NVT ensemble, averaging eq. 4 over a MD run and normalizing with the maximum value. This provides an estimation of the effect

of constraints over statistical averages such as used in eq. 4, to carry out the thermodynamic integration. We got the following main difference between the constrained and unconstrained probabilities at $T = 300K$:

$$\frac{\rho}{\rho_{constrained}} \sim \left\langle \sqrt{|Z|} \right\rangle \sim 0.954\,.$$

The closeness to 1 indicates that the effect of bond constrains is practically negligible for simulations in the studied range of thermodynamic variables. From this estimation we can conclude that the points obtained in figure 2 are almost identical to those that can be obtained in a similar simulation without bond constrains, that would have been quite more expensive in CPU time. This simple calculation, that we present here for close ring-molecules, is complementary to that already obtained in ref. [31] for open chain molecules.

**Contribution of stretching modes to free energy**

We include here an estimation of the free energy difference between samples with and without molecular bond constrains, under the framework of quasi-harmonic approximation commented in sec. II B. If we think in the normal modes as harmonic oscillators of frequency $\nu_i$, we have a 'trivial' partition function $Z_i$ for each oscillator of the form[17]:

$$Z_i = e^{-i\frac{1}{2}h\nu_i} \sum_{s=0}^{\infty} e^{-sh\nu_i/kT} = \frac{e^{-i\frac{1}{2}h\nu_i}}{1-e^{-ih\nu_i}}$$

where $h$ is the Planck constant, $k$ the Boltzmann factor and $s$ the positive integer quantum number of the oscillator of frequency $\nu_i$. For a system of such independent oscillators we have a partition function:

$$Q_{simul} = \int_0^{\infty} D(\nu)\left(\frac{e^{-\frac{1}{2}\beta h\nu}}{1-e^{-\beta h\nu}}\right) d\nu\,, \tag{5}$$

where $D(\nu)$ is the density of vibrational states already defined in sec. II B and $Q_{simul}$ is calculated from our bond constrained MD simulation. The partition function of the unconstrained system $Q$ can be estimated in the following way: taking into account that for the $S_8$ molecule the stretching vibrational modes are well above bending and torsional modes in the $\nu$ scale (see sec. III), we have separable contributions for the total partition function of the molecule and

$$Q = \int_0^{\nu_{max}} D_{simul}(\nu)\left(\frac{e^{-\frac{1}{2}\beta h\nu}}{1-e^{-\beta h\nu}}\right) d\nu + \int_{\nu_{max}}^{\infty} D_{stretch}(\nu)\left(\frac{e^{-\frac{1}{2}\beta h\nu}}{1-e^{-\beta h\nu}}\right) d\nu \equiv Q_{simul} + Q_{stretch}, \tag{6}$$

where we have assumed that the interval $(0, \nu_{max})$ accounts for the bending, torsional (dihedral) and lattice vibration modes and the high frequencies of bond stretching are 'isolated' in the interval $(\nu_{max}, \infty)$. The first term in eq. 6 is obtained from our simulation and the second one can be simply approximated by:

$$Q_{stretch} = N^{stretch}\left(\frac{e^{-\frac{1}{2}\beta h\nu_{stretch}}}{1-e^{-\beta h\nu_{stretch}}}\right),$$

here $N^{stretch}$ are the 8 stretching degrees of freedom (constrained in the MD simulations) and $\nu_{stretch}$ is the mean stretching frequency. This is equivalent to use the relationship $D_{stretch}(\nu) = N^{stretch} \times \delta(\nu - \nu_{stretch})$. The free energy difference between considering or not the stretching degrees of freedom can be estimated, under the quasi-harmonic approximation by:

$$\beta\Delta F = \beta(F_{tot} - F_{simul}) = \ln\left(\frac{Q_{simul}}{Q_{simul} + Q_{stretch}}\right)$$

For $T = 300K$ and the sulphur mean stretching frequency $\nu_{stretch} = 453.8\,cm^{-1}$, we get $\beta\Delta F = 0.075$ which is a relatively and also an absolute small number when compared with the $\beta F$ values of table I.

This simple calculation can be considered complementary to those of ref. [19, 20, 21], that provided a thorough discussion of the role of bond constrains in free energy calculations.

---


[1] D. Frenkel, A. J. C. Ladd, *J. Chem. Phys.*, *J. Chem. Phys.* **81** *p.* 3188 (1984)

[2] Steudel R., Chemie unserer Zeit **30**, 226 (1996).

[3] Meyer B., Chem. Rev. **76**, 367 (1976).

[4] Montgomery R. L., Science **184**, 562 (1974).

[5] Sands D. E., J. Am. Chem. Soc. **87**, 1396 (1965).

[6] C. Pastorino, Z. Gamba, *J. Chem. Phys.* **112** p.282 *(2000)*

[7] C. Pastorino, Z. Gamba, *Chem. Phys. Lett.* **319** p.20 (2000)

[8] Venuti E., Cardini G. and Castellucci E., Chem. Phys. **165**, 313 (1992).

[9] B. Eckert, R. Schumacher, H. J. Jodl and P. Foggi, High Pressure Research **17**, 773 (1999) and personal communications.

[10] J. Wallis, I. Sigalas and S. Hart, J. Appl. Cryst. **19**, 273 (1986).

[11] C. Pastorino, Z. Gamba, *Chem. Phys.* **261** (3) p.317 (2000) ; idd. , *Chem. Phys.* **273**, 73 (2001)

[12] M. W. Schmidt, K. K. Baldridge, J. A. Boatz, S. T. Elbert, M. S. Gordon, J. H. Jensen, S. Koseki, N. Matsunaga, K. A. Nguyen, S. J. Su, T. L. Windus, M. Dupuis, J. A. Montgomery, J. Comp. Chem. 14, 1347 (1993)

[13] Coppens P., Yang Y. W., Blessing R. H., Cooper W. F. and Larsen F. K., J. Am. Chem. Soc. **99**, 760 (1977).

[14] C. Pastorino, Z. Gamba, *J. Chem. Phys.* **115** p. 9421 (2001)

[15] J. M. Polson, E. Trizac, S. Pronk and D. Frenkel, *J. Chem. Phys.*, **112** p. 5339 (2000).

[16] B. Smit, D. Frenkel, *Understanding Molecular Simulations, Academic Press* (1996)

[17] Born M. and Huang K. "Dynamical Theory of crystal lattices". Oxford, Clarendon Press, New York, 1954, p. 39.

[18] J. Polson, D. Frenkel, J. Chem. Phys. **109** p.318 (1998)

[19] D. A. Pearlman, P. A. Kollman, *J. Chem. Phys* **94**, 4532 (1991)

[20] T. P. Straatsma, M. Zacharias, J. A McCammon, *Chem. Phys. Lett.* **196**, 297 (1992)

[21] D. A. Pearlman, *J. Chem. Phys.*, **98,** 8946 (1992)

[22] M. P. Allen, D. J. Tildesley, *Molecular simulations of liquids*, Clarendon Press, Oxford (1990)

[23] G. J. Martyna, M. L. Klein, M. Tuckerman, J. Chem. Phys. ***97*** p. 2635 (1992)

[24] Nosé, J. Chem. Phys. **81**, 511 (1984)

[25] W. G. Hoover, Phys Rev A **31**, p. 1695 (1985)

[26] J. Polson, D. Frenkel, J. Chem. Phys. **111** p.1501 (1999)

[27] W. K. Den Otter and W. J. Briels, Mol. Phys. **98**, 773 (2000).

[28] J. P. Ryckaert, S. Ciccotti, *J. Chem. Phys.* **78** 7368 (1983)

[29] E. Darve, A. Pohorille, *J. Chem. Phys.* **115**, 9196 (2001)

[30] E. A. Carter, G. Ciccotti, J. T. Hynes, R. Kapral *Chem. Phys. Lett.* **156**, 472 (1989)

[31] M. Fixman *Proc. Nat. Acad. Sci.* **71,** 3050 (1974).